Cell, Vol. 109, 599–610, May 31, 2002, Copyright ©2002 by Cell Press

Tumor Suppressor PTEN Mediates Sensing of Chemoattractant Gradients

Miho Iijima and Peter Devreotes[1]
Department of Cell Biology
Johns Hopkins University
School of Medicine
Baltimore, Maryland 21205

Summary

Shallow gradients of chemoattractants, sensed by G protein-linked signaling pathways, elicit localized binding of PH domains specific for $PI(3,4,5)P_3$ at sites on the membrane where rearrangements of the cytoskeleton and pseudopod extension occur. Disruption of the PI 3-phosphatase, PTEN, in *Dictyostelium discoideum* dramatically prolonged and broadened the PH domain relocation and actin polymerization responses, causing the cells lacking PTEN to follow a circuitous route toward the attractant. Exogenously expressed PTEN-GFP localized to the surface membrane at the rear of the cell. Membrane localization required a putative $PI(4,5)P_2$ binding motif and was required for chemotaxis. These results suggest that specific phosphoinositides direct actin polymerization to the cell's leading edge and regulation of PTEN through a feedback loop plays a critical role in gradient sensing and directional migration.

Introduction

Many cells have a biochemical compass that allows them to sense the direction of extracellular stimuli and guides their movements along chemoattractant gradients (Parent and Devreotes, 1999; Rickert et al., 2000). This process, called chemotaxis, plays a role in normal physiological events such as lymphocyte homing, angiogenesis, embryogenesis, and wound healing and in diseases such as asthma, multiple sclerosis, arthritis, and cancer (Wardlaw et al., 2000; Baggiolini, 2001). In many instances, the chemoattractants are detected by G protein-coupled receptors, which control numerous cellular processes including cell polarization—chemotactic cells are typically elongated and more sensitive to attractant at one end—and directional sensing, relatively unpolarized cells are able to detect shallow external gradients. A current challenge is to elucidate the signal transduction events that mediate cell polarization and directional sensing, which together comprise the cell's compass.

Studies in *Dictyostelium discoideum* and in mammalian leukocytes have shown that chemoattractant receptors and G protein subunits remain distributed uniformly on the perimeter of a chemotaxing cell and therefore, the signaling pathways must be selectively activated on the cell's leading edge (Xiao et al., 1997; Servant et al., 1999). In an experiment that first visualized localized activation, the PH domain of *c*ytosolic *r*egulator of *a*denylyl *c*yclase (Crac) was shown to selectively translocate to the membrane at the front of a chemotaxing *D. discoideum* cell (Parent et al., 1998; Jin et al., 2000). It is likely that Crac is recruited to the membrane by binding to specific phosphoinositides (Y.E. Huang and P.D., unpublished data). Other PH domains with the same phosphoinositide binding specificity as Crac have subsequently been shown to respond similarly to chemoattractants in *D. discoideum* and leukocytes (Meili et al., 1999; Haugh et al., 2000; Servant et al., 2000). The profile of PH domains which report the directional response most effectively suggests changes occur in the local concentrations of phosphatidylinositol 3,4,5 trisphosphate ($PI(3,4,5)P_3$) and phosphatidylinositol 3,4 bisphosphate ($PI(3,4)P_2$). These observations led to the proposal that the determination of the directional response occurs within the signaling pathway and that the activity of the cytoskeleton is locally controlled by these phosphoinositides (Parent et al., 1998).

Exposure of cells to a uniform increment in chemoattractant results in transient increases in phosphoinositides, polymerized actin, cAMP, cGMP, IP_3, and Ca^{+2} influx, phosphorylation of myosins as well as rapid changes in cell shape (van Es and Devreotes, 1999). Evidence suggests that the G protein $\beta\gamma$ complex propagates the signal to these responses, although the identities of its direct and relevant effectors are unknown. It is possible that the G protein couples to only a few effector enzymes and that an increase in a single messenger regulates multiple downstream responses. In fact, many responses display similar kinetics and several are known to occur at the leading edge of the cell, suggesting a level of coordination. We have proposed that specific phosphoinositides act as a "node" in the chemoattractant signaling pathway and that downstream components bearing PH domains and involved in pseudopodia extension are directed to the site on the membrane marked by highest concentration of these lipids (Parent et al., 1998).

Thus far, a causal relationship between the elicited appearance of specific phosphoinositides, actin polymerization, other physiological responses, and directional pseudopod extension has not been established. Evidence suggesting a role of phosphatidylinositol 3-kinases (PI3K) in directed migration has been confusing. *D. discoideum* cells lacking multiple PI3Ks have alternately been described as displaying either faster or impaired chemotaxis (Buczynski et al., 1997; Funamoto et al., 2001). Neutrophils from mice lacking PI3Kγ show defective chemotaxis, while lymphocytes do not show strong defects (Hirsch et al., 2000; Li et al., 2000; Sasaki et al., 2000). Similarly, inconsistent results have been obtained with the PI3K inhibitors, LY294002 and wortmannin, which have been reported to either inhibit or have little effect on chemotaxis (Wu et al., 2000a; Wymann et al., 2000). Furthermore, actin polymerization, the salient response underlying pseudopod extension, is unaffected by mutations or inhibitors of PI3K. Disruption of the PI 3-phophatase, PTEN, and the PI 5-phosphatase, SHIP, in mice, *D. melanogaster*, and *C. elegans*

[1]Correspondence: pnd@jhmi.edu

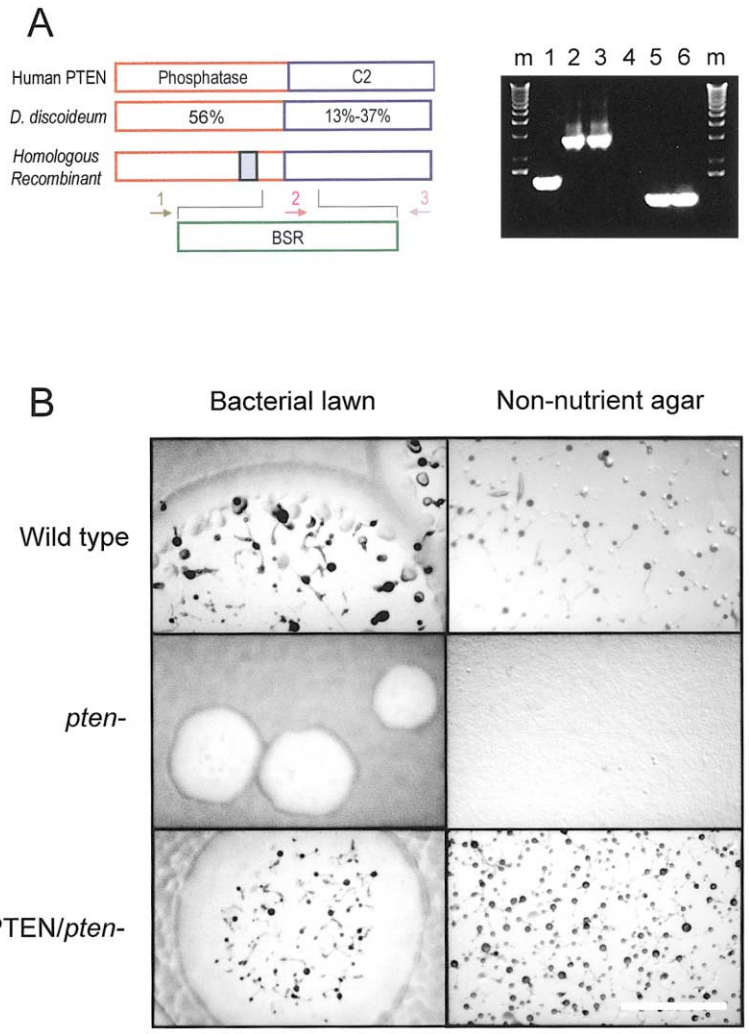

Figure 1. PTEN Ortholog and Disruption

(A) A Blasticidin resistance marker (BSR) was inserted into the Hinc II site of the PTEN gene by homologous recombination as shown. The gray box represents the active site of the phosphatase domain. In the PCR analysis, lanes 1–3 show bands from primer pair 1:3 on genomic DNA from wild-type and two *pten*$^-$ clones. Lanes 4–6 show bands from primer pair 2:3 on same genomic DNA preparations. Primers 1 and 3 are in the PTEN sequence; primer 2 is in BSR sequence. The sequences of primers 1, 2, and 3 are 5′-GCAATGGGATT TCCAAGTGAAAAGTTG-3′, 5′-GCATTGTAAT CTTCTCTGTCGCTAC-3′ and 5′-GAGCTATT TGAAGAAGTTTCACTGTC-3′. Marker lanes show the 1 Kb DNA ladder (GIBCO).

(B) Phenotypes of wild-type, *pten*$^-$, and PTEN-GFP/*pten*$^-$ cells as clonal plaques on bacterial lawns and on nonnutrient agar. Cells within wild-type plaques (top) differentiate and aggregate to form multicellular fruiting bodies. The *pten*$^-$ cells (middle) form smaller plaques and the cells fail to aggregate. Expression of PTEN-GFP in the *pten*$^-$ cells nearly restores the wild-type phenotype. Calibration bar indicates 3 mm. Supplemental Video S1B, available at http://www.cell.com/cgi/content/full/109/5/599/DC1, of *pten*$^-$, and PTEN-GFP/*pten*$^-$ cells aggregating on nonnutrient agar were recorded by phase contrast microscopy at 100-fold magnification. Time-lapse ratio was 240-fold.

has been reported to cause dramatic pleiotropic phenotypes, including reports of enhanced cytoskeletal activity (Ogg and Ruvkun, 1998; Stambolic et al., 1998; Goberdhan et al., 1999; Kim et al., 1999). However, effects on motility and chemotaxis have not been assessed. The roles of PTEN in cell polarization, directional sensing, or actin polymerization remain to be defined. We reasoned that investigation of PTEN in a biochemically and microscopically accessible cell, such as *D. discoideum*, would clearly elucidate the link between these lipids, the physiological responses triggered by chemoattractants, and directional sensing.

Results

Isolation and Disruption of an Ortholog of the PI 3-Phosphatase and Tumor Suppressor PTEN

To interfere with the regulation of PI(3,4,5)P_3 and PI(3,4)P_2, we sought and disrupted by homologous recombination a putative PI 3-phosphatase in *D. discoideum*. A genomic search revealed seven sequences with protein tyrosine phosphatase (PTP) motifs, but only one gene stood out as a bona fide ortholog of the human PTEN tumor suppressor gene. As illustrated in Figure 1A, the N-terminal half of the PTEN gene containing the phosphatase domain is 56% identical to the human gene. The C-terminal regions containing the C2, PEST, and PDZ domains in the mammalian enzyme are 13% to 37% identical (Maehama et al., 2001). We inserted a blasticidin resistance marker into the open reading frame, transformed cells, and screened for homologous recombination events by PCR and Southern analysis. Several positive clones were found in a search of over 1200 drug-resistant colonies from six independent transformations. As shown in Figure 1A, specific primer sets showed bands of the expected size in *pten*$^-$ and wild-type clones. Southern blots showed that several copies of the plasmid had inserted into a single site within the PTEN locus (data not shown). The extremely low efficiency of gene disruption is attributed to the slow growth rate of the disruptants. In axenic HL-5 medium, the *pten*$^-$ cells have a doubling time of 25 hr versus 11 hr for the wild-type. The origin of the slower growth rate is under investigation. All of the phenotypes of the *pten*$^-$ cells including the growth defect were reversed by expression of the full-length PTEN cDNA from a constitutively active promoter. The PTEN/*pten*$^-$ as well as wild-type cells were used as controls in subsequent characterization of the *pten*$^-$ cells.

The wild-type, *pten*$^-$, and PTEN/*pten*$^-$ cells display

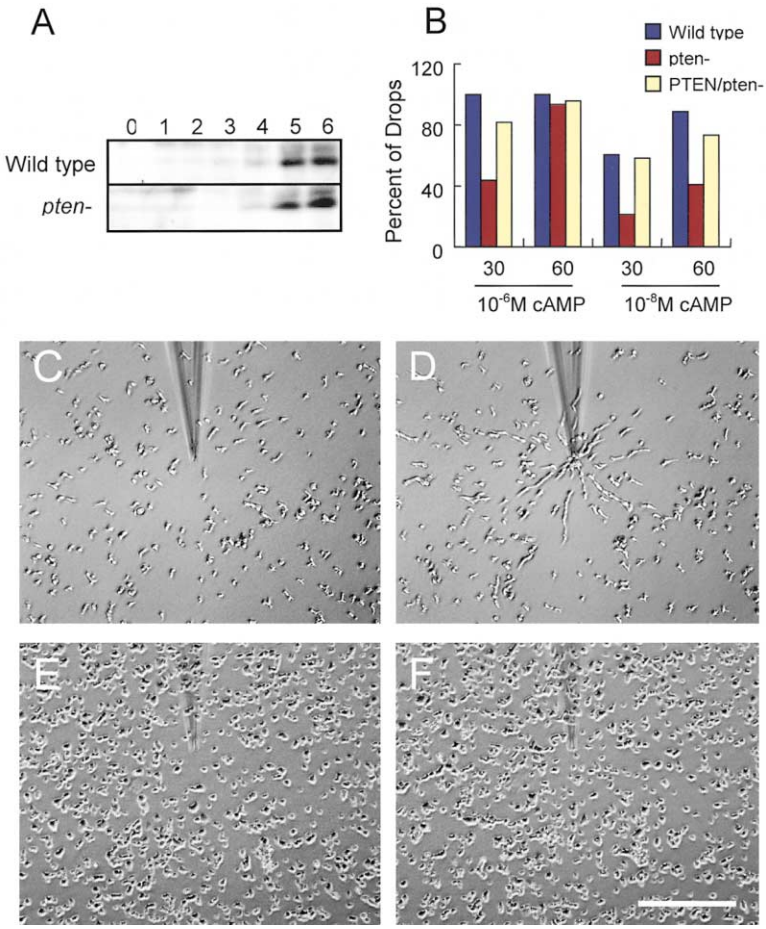

Figure 2. Expression of cAMP Receptor cAR1 and Chemotactic Responses

(A) Immunoblot of the major cAMP receptor cAR1 in wild-type and *pten*$^-$ cells differentiated for 0, 1, 2, 3, 4, 5, and 6 hr.

(B) The response of wild-type, *pten*$^-$, and PTEN-GFP/*pten*$^-$ cells to 10^{-6} or 10^{-8} M cAMP was examined using the small-drop assay. After 30 or 60 min, over 200 drops were judged and the percentage positive drops were scored.

(C–F) Chemotaxis to a micropitette filled with 1 μM cAMP. The movement of wild-type, *pten*$^-$ (E and F), or PTEN-GFP/*pten*$^-$ (C and D) cells was recorded. The photographs of 0 (C and E) and 20 (D and F) min are shown. Calibration bar indicates 0.4 mm.

dramatically different developmental phenotypes. When starved, *D. discoideum* cells spontaneously aggregate and differentiate to form beautifully patterned multicellular structures. Aggregation is brought about by propagated waves of cAMP, which emanate from centers at 6 min intervals and coordinate periodic steps of chemotactic cell motion. The *pten*$^-$ cells failed to aggregate under a variety of conditions suggesting a strong defect in chemotaxis or cell-cell signaling (Figure 1B). On bacterial lawns, individual cells formed small plaques, suggesting an additional defect in growth or phagocytosis (Figure 1B). Time-lapse video analysis of the *pten*$^-$ cells plated on nonnutrient agar showed that cell-cell signaling starts normally within a few hours of the onset of development (Figure 1B and Supplemental Video S1B, available at http://www.cell.com/cgi/content/full/109/5/599/DC1). Consistently the major chemoattractant receptor, cAR1, appeared at the 5 to 6 hr stage at the same level in both wild-type and *pten*$^-$ cells (Figure 2A). However, the typically rhythmic waves of cell motion reflecting cell-cell signaling were unstable. New centers appeared throughout the field as existing centers failed to persist, suggesting that the oscillations in cAMP production are unsustainable (see Videos 1B). Moreover, while the cells did react to the cAMP waves by changing shape, their chemotactic steps toward the center were much less significant than those of wild-type cells. The *pten*$^-$ cells eventually formed a few tiny deformed multicellular structures. Thus, in spite of clear evidence of appropriate differentiation and onset of cell-cell signaling, aggregation does not occur normally. The PTEN/*pten*$^-$ cells displayed large aggregation positive plaques on bacterial lawns and formed normal fruiting bodies on nonnutrient agar, indicating that the defects in the *pten*$^-$ cells are specifically due to the absence of PTEN (Figure 1B).

The failure of the *pten*$^-$ cells to aggregate can be traced to multiple interesting deficiencies. Chemotaxis is very defective as determined in standard small drop and micropipette assays. In the small drop assay, spots of a few hundred cells are placed near spots of cAMP on an agar surface (Figure 2B). Wild-type cells typically show directed movement toward the chemoattractant at concentrations ranging from 10 nM to 10 μM. The *pten*$^-$ cells responded more slowly and less vigorously than wild-type cells. Whereas all of the spots of wild-type cells scored as positive within 15 to 30 min, only a fraction of the spots of the *pten*$^-$ cells scored positive at 30 min. In steeper gradients after 60 to 90 min, *pten*$^-$ cells did score positively. In the micropippette assay, a needle releasing chemoattractant is placed in a field of cells and establishes a 10% gradient along the length of a typical cell. Within 20 min, wild-type (not shown) or PTEN/*pten*$^-$ cells gather at the tip. The *pten*$^-$ cells display only a barely detectable accumulation under the same conditions (Figures 2C–2F). The *pten*$^-$ cells dis-

play numerous long filopodia and extend pseudopodia more rapidly and erratically than the wild-type cells, possibly accounting for the slower rate of accumulation toward chemoattractant (see below). The PTEN/*pten*$^-$ cells regained the normal morphological appearance as well as the rapid chemotactic responses of the wild-type cells.

Chemoattractant-Elicited Changes in PH Domains, Actin Polymerization, and Cyclic Nucleotides in Pten$^-$ Cells

We expressed the PH domain of Crac fused to green fluorescent protein (PH_{Crac}-GFP) in *pten*$^-$ cells and monitored chemoattractant-induced production of PH domain binding sites on the plasma membrane by subcellular fractionation and fluorescence microscopy (Figure 3 and Supplemental Videos S3B, top and bottom, available at http://www.cell.com/cgi/content/full/109/5/599/DC1). When an incremental stimulus was applied to wild-type cells, the fusion protein rapidly translocated to the membrane and returned to the cytosol within 20 to 60 s. In *pten*$^-$ cells, the translocation of PH_{Crac}-GFP to the membrane was dramatically exaggerated and prolonged. The maximal levels associated with the membrane were slightly higher; and after 180 s, significant amounts still remained associated with the membrane. Eventually after 6 to 8 min, the response subsided (data not shown). Moreover, significantly lower doses of chemoattractant were required to elicit an equivalent response in the *pten*$^-$ versus wild-type cells. Whereas 1 nM was needed for a clear response in wild-type cells, a similar response in the *pten*$^-$ cells was observed with 10 pM cAMP (data not shown). This concentration is calculated to occupy about twenty receptors per cell, suggesting that there is significant amplification of the response, which is normally regulated down by PTEN in wild-type cells. We also compared the PH domain translocation responses induced by added cAMP to those elicited by folic acid, a chemoattractant active on growth stage cells, which acts through different receptors and heterotrimeric G proteins. Uniform increases in folic acid elicited prolonged responses in the *pten*$^-$ versus wild-type cells; however, the differences were less pronounced (not shown).

The features of chemoattractant-induced actin polymerization in wild-type versus *pten*$^-$ cells differ dramatically (Figure 4). In wild-type cells, stimulation typically triggers a biphasic response. An initial large peak occurs at 6 s; it is followed by a rapid decrease and a subsequent broad low peak centered at 2 min. In the *pten*$^-$ cells, the basal level of polymerized actin typically was about 30% higher than that in wild-type cells. This elevated level may underlie the increased frequency of spontaneous protrusions observed in unstimulated cells. Stimulation with cAMP triggered larger and apparently longer increases in actin polymerization in the *pten*$^-$ versus wild-type cells. The differences were most evident in the second peak, which was significantly exaggerated (Figure 4A). In four independent experiments, the F actin levels at 1 and 2 min were typically 6-fold higher in the *pten*$^-$ versus wild-type cells. Whereas the response in wild-type cells was barely detectable at 3 min, the response of the *pten*$^-$ cells remained elevated even after 5 min of stimulation. During stimulation, the *pten*$^-$ cells periodically extended numerous actin-rich projections, including filopods and elongated pseudopodia (see Figure 3). We compared the PH-GFP relocation and actin polymerization responses by fluorescence microscopy at 30 s when the wild-type responses had nearly subsided. As shown in Figure 4C, in the *pten*$^-$ cells the regions on the membrane where the PH-GFP signal persisted coincided with those of higher F actin accumulation. Eventually after about 10 min of continuous stimulation, the response of the *pten*$^-$ cells appeared to subside. A normal actin polymerization response similar to that in wild-type cells was restored in the PTEN/*pten*$^-$ cells (Figure 4A).

We next monitored the cAMP-induced increases in cyclic nucleotides cAMP and cGMP in the *pten*$^-$ versus wild-type cells. In wild-type cells, a transient increase in adenylyl cyclase can be monitored in lysates prepared from cells sampled before and after stimulation. The response underlies the oscillatory production of cAMP and propagated waves of cAMP, which coordinate chemotactic movements of cells during aggregation. As shown in Figure 5, the elicited level of activation of adenylyl cyclase 1 min after stimulus addition was 2- to 4-fold higher in the *pten*$^-$ versus wild-type cells in five independent experiments. The time-course of the adenylyl cyclase response, however, was not significantly prolonged in the *pten*$^-$ cells. Expression of PTEN in the *pten*$^-$ cells restored the smaller response typically observed in wild-type cells. In wild-type cells, the chemoattractants folic acid and cAMP each trigger rapid accumulations of cGMP which peak within 10 s and return toward baseline levels by 30 to 60 s (Figure 5). The cGMP accumulation responses elicited by cAMP were not significantly different in the *pten*$^-$ versus wild-type cells.

Altered Levels of Phosphosinositides Lead to Chemotaxis Defects

We examined the chemotactic defects in finer detail by observing the responses of wild-type and *pten*$^-$ cells to gradients supplied by chemoattractant-filled micropipettes. As shown in Figure 6 and corresponding videos, the wild-type cells maintained a persistently focused leading edge that facilitated their movement directly toward the source of the chemoattractant. In contrast, the *pten*$^-$ cells displayed a broad irregular front, often the *pten*$^-$ cells extended three or more pseudopodia pointing generally but not directly up the gradient. Occasionally, pseudopodia appeared at the rear of the cell and the cell moved backward. Thus, compared to wild-type cells, the *pten*$^-$ cells followed a more circuitous path toward the source of the attractant (Figure 6). The mean speed and chemotactic indices of the *pten*$^-$ cells were 3.0 ± 1.3 μm/min and 0.79 ± 0.46, respectively. These values for the wild-type cells were 11.4 ± 3.6 μm/min and 0.99 ± 0.01. This behavior explains the weaker chemotactic responses observed in the small drop and micropipette assays described earlier.

To understand this defective chemotactic response, we examined the distribution of the PH domains in the *pten*$^-$ versus wild-type cells. We expressed PH_{Crac}-GFP in wild-type and *pten*$^-$ cells and observed the distribu-

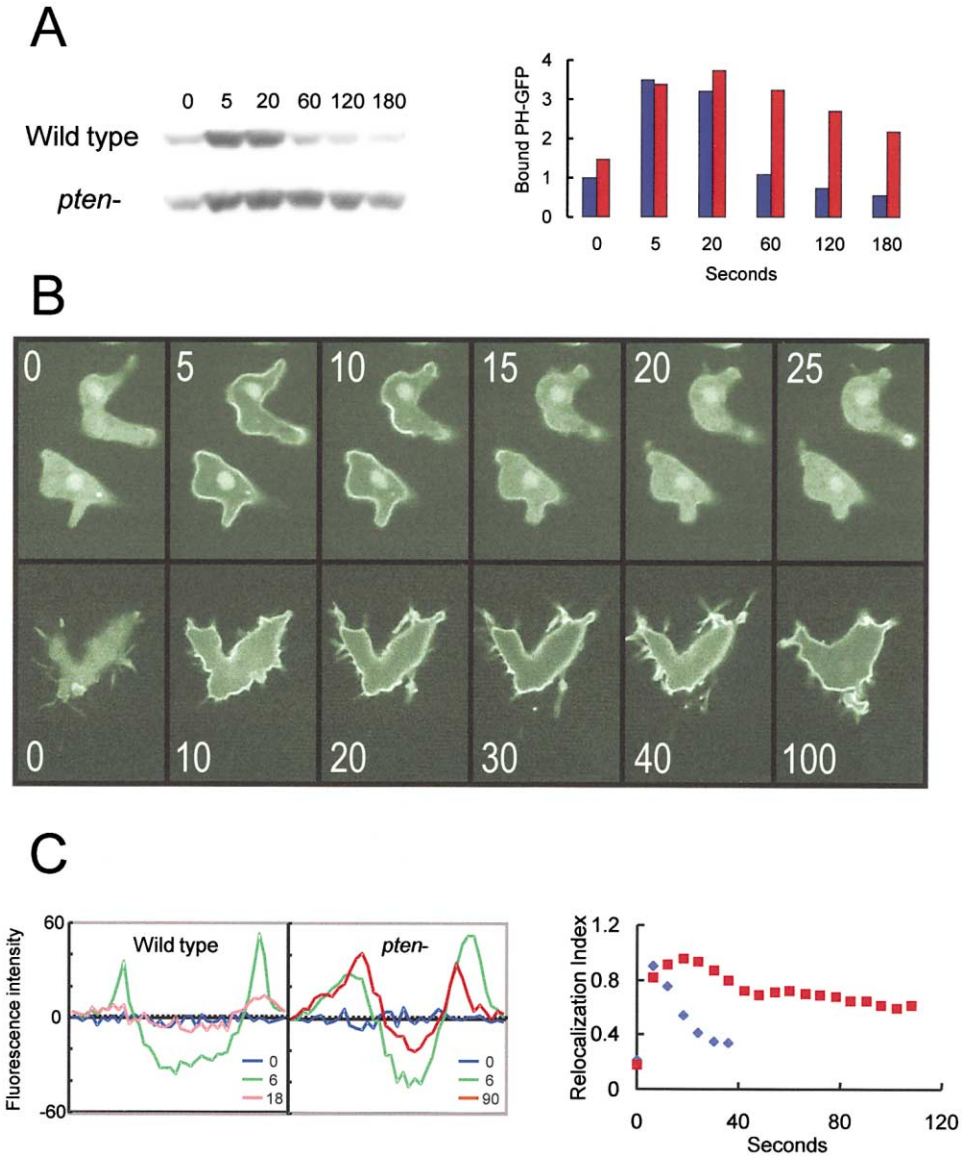

Figure 3. PH_{Crac}-GFP Translocation in Wild-Type and *pten*$^-$ Cells

(A) Suspensions of wild-type or *pten*$^-$ cells expressing PH_{Crac}-GFP were stimulated with 1 μM cAMP. At each of the indicated time points (seconds), aliquots of cells were lysed into buffer and membranes were collected by microcentrifugation. The bound PH_{Crac}-GFP was analyzed by immunoblot detection of GFP. The relative amounts of the PH_{Crac}-GFP associated with membrane fraction were quantified using NIH Image software. Blue bars are wild-type cells; red bars are *pten*$^-$ cells.

(B) Confocal images captured at the indicated times (seconds) following addition of 100 nM cAMP. Top, response in wild-type cells returns completely to baseline within 25 s. Bottom, response in *pten*$^-$ cells declines with a half time of several minutes. Supplemental Videos S3B top and bottom available at http://www.cell.com/cgi/content/full/109/5/599/DC1 show a complete sequence from which timed images were taken. Single white frame in video indicates the addition of a stimulus increment. Images were captured at 3 s intervals and played back at 0.2 s intervals.

(C) Quantitative analysis of the PH_{Crac}-GFP translocation. Fluorescence intensity was measured by scanning a line through a cell with IPLab software. The change of fluorescence distribution was calculated by subtracting the intensity along the line before stimulation from the intensity along the same line at the indicated times. To reveal the kinetics of the PH_{Crac}-GFP translocation after cAMP stimulation, for each time point the sum of the increase at the membrane and the decrease in the cytosol were determined, and all the data were normalized to the maximal level observed in the *pten*$^-$ cells (right). This normalized sum was designated "Relocalization Index." Average data from 12 wild-type (blue) or pten$^-$ (red) cells in separate experiments are shown.

tions in cells exposed to gradients supplied by a micropipette. As shown in Figures 6C and 6D and Supplementary Videos S6C and S6D, the multiple misdirected pseudopods extended by the chemotaxing *pten*$^-$ cells are simultaneously labeled with PH_{Crac}-GFP. At any moment, an extensively broader region along the leading edge of the cell is associated with the PH_{Crac}-GFP. In still images of wild-type cells, an average of 9.5% ± 2% of the perimeter was covered by PH_{Crac}-GFP, while in *pten*$^-$ cells 47% ± 8% of the perimeter was occupied.

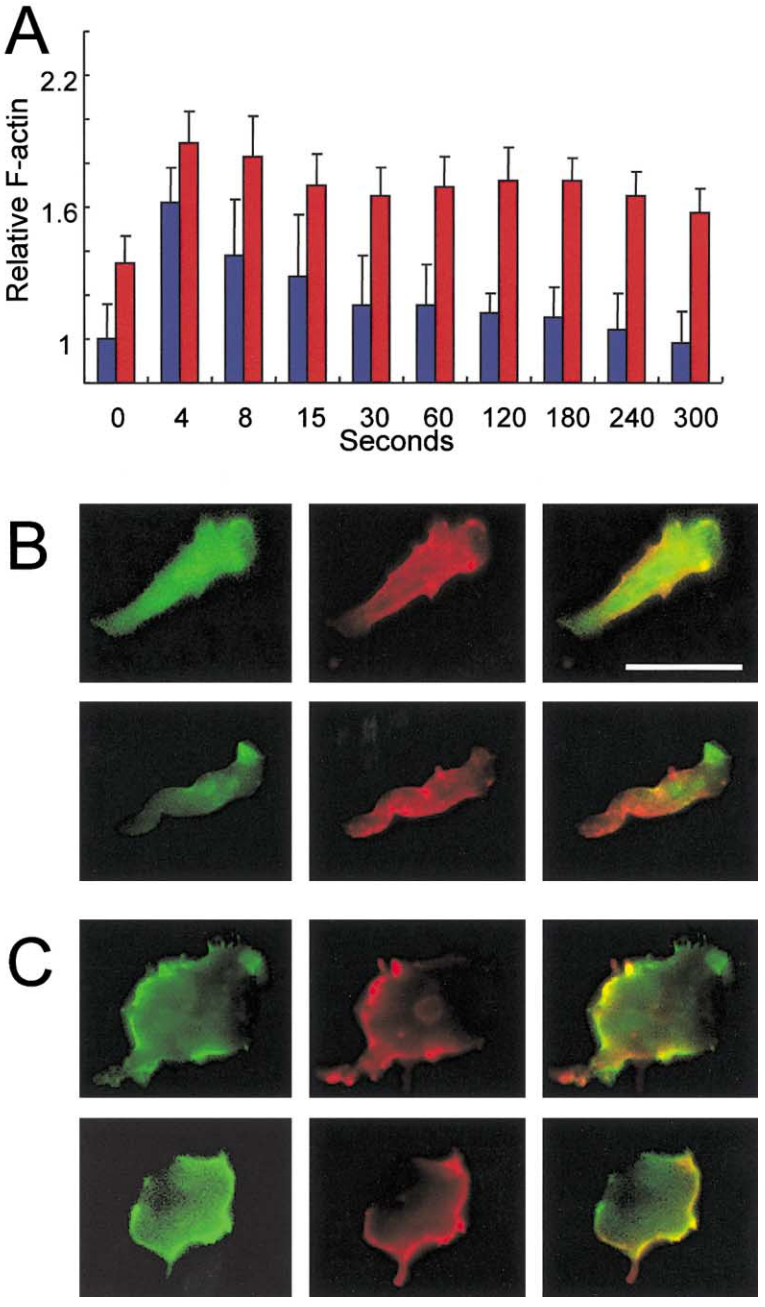

Figure 4. Prolonged and Exaggerated Actin Polymerization in *pten*$^-$ Cells

(A) The t = 0 sample was taken before addition of a 1 μM cAMP stimulus. Values are normalized to the amount of F actin in wild-type cells at t = 0. This typically corresponds to about 30% of the total actin pool. There was no difference in the total actin levels in the wild-type versus *pten*$^-$ cells. The data shown are means of at least four independent experiments. Blue bars are wild-type cells; red bars are *pten*$^-$ cells.

(B and C) Wild-type (B) and *pten*$^-$ (C) cells were stimulated with 1 μM cAMP. After 30 s, cells were fixed with 2% parafomaldehyde/0.1% triton and stained with TRITC-Phalloidin. Two typical cells are shown for each cell type. Green is PH-GFP, red is RITC-phalloidin, and the merged image is shown at right.

In addition, many of the *pten*$^-$ cells displayed a region of PH_{Crac}-GFP at the rear of the cell. This region occasionally expanded and the cell then extended a pseudopod toward the back (Figure 6D).

We next examined the distribution of PTEN-GFP in living cells during chemotactic stimulation. PTEN-GFP was functional since, as described above, it rescued all of the phenotypes of the *pten*$^-$ cells. In resting cells, about 4% of the fluorescent signal was associated with the perimeter of the cell while the remainder was distributed uniformly in the cytosol (Figure 7). When a uniform increase in extracellular cAMP was applied to the cells, 94% of the bound PTEN-GFP rapidly dissociated from the membrane. Within 1 min of continuous stimulation, the protein returned to the membrane. Often the level of membrane association in the adapted cells reached 10% and thus exceeded that of the unstimulated cells (Figure 7A). When cells were exposed to a gradient from a cAMP-filled micropipette, the PTEN-GFP dissociated from the leading edge and accumulated at the rear of the cell (Figure 7B and Supplemental Video S7, available at http://www.cell.com/cgi/content/full/109/5/599/DC1)

To investigate the mechanism of association of PTEN with the membrane, we deleted the putative $PI(4,5)P_2$ binding domain, located in the N-terminal of the protein. Removal of the 16 amino acids, containing this site, resulted in a PTEN-GFP protein that no longer associated with the membrane. Instead, all of the protein was localized uniformly in the cytosol with a distribution essentially identical to that of GFP (Figure 7C). Subcellular

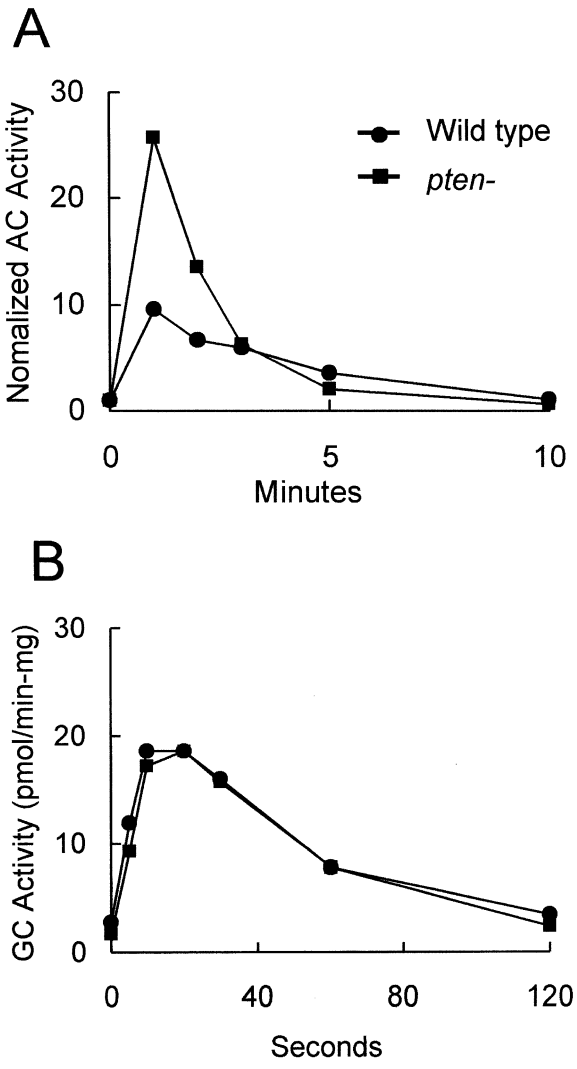

Figure 5. Chemoattractant-Elicited Changes in Cyclic Nucleotides

(A) Adenylyl cyclase activity was determined from lysates prepared before and after 1 μM cAMP stimulation. Experiment was repeated five times with similar fold increases for wild-type and *pten*$^-$ cells and the averages of normalized activities are shown. For each experiment, activities were normalized to the prestimulus value of the wild-type cells. The peak activity in wild-type was typically 10–20 pmoles/min/mg.

(B) cGMP levels in cells prepared during 1 μM cAMP stimulation. Experiment was repeated at least three times with similar results, and the averages of cGMP levels are shown.

fractionation and immunoblot analyses also indicated that the amount of PTEN-GFP associated with the membrane was reduced (data not shown). Interestingly, the cytosolic version of PTEN-GFP was unable to rescue the *pten*$^-$ cells, suggesting that membrane localization is required for the function of PTEN in chemotaxis (data not shown).

Discussion

We have previously proposed that detection of the external gradient and localization of the response to the front of the cell first occurs within the signal transduction pathway (Parent et al., 1998). The restricted response is visualized with GFP-tagged PH domains which specifically detect PI(3,4,5)P_3 or PI(3,4)P_2 in living cells. We further suggested that physiological responses such as actin polymerization, which bring about pseudopod extension, are directed to sites on the inner face of the membrane with the highest concentration of these phosphoinositides. The observations of the *pten*$^-$ cells confirm and extend these proposals and establish a working model for directional sensing. This advance allows future studies to focus on two key questions: First, how does phosphoinositide production become limited to the front edge of the cell? Second, what are the steps linking the increased phosphoinositides to pseudopod extension?

We have outlined a local excitation and global inhibition model for localizing the response to an external gradient (Parent and Devreotes, 1999). This model has been extended and quantitatively analyzed (Levchenko and Iglesias, 2002). Briefly, a balance between the rapid excitatory and the slower inhibitory processes, which are each controlled by receptor occupancy, regulates the response. When receptor occupancy is changed and then held constant, excitation rapidly increases and a response ensues until inhibition eventually attains the same level. In a spatial gradient, the steady-state level of excitation at the front of the cell exceeds the level of global inhibition and there is a persistent response. At the back, excitation is less than inhibition so there is no response. According to this model, the duration of a response to a stimulus increment is related to its spatial localization in a gradient. Responses of brief duration are tightly localized, while those that do not subside cannot be sharply confined. The observations on the *pten*$^-$ cells are consistent with this aspect of the model. In the *pten*$^-$ cells, there is an increase in the duration of the response to a stimulus increment and a corresponding broadening of the localization of the phosphoinositides in a gradient. Recent observations of G protein signaling in living cells using fluorescence resonance energy transfer (FRET) have shown that the G protein subunits remain disassociated as long as receptors are occupied and thus the activated G protein is not expected to be localized (Janetopoulos et al., 2001). This suggests that there is a receptor-mediated inhibitory process that acts downstream of the G protein cycle to terminate the physiological responses and offset G protein activation at the back of the cell.

The observations of *pten*$^-$ cells demonstrate that there is a causal link between PI(3,4,5)P_3 and PI(3,4)P_2 regulation, actin polymerization, and chemotactic response. Whereas previous studies have illustrated a temporal and spatial correlation between these lipids and the physiological responses underlying pseudopodia formation, the results reported here show a direct, ordered relationship. In response to stimulus increments, the magnitude and time course of phosphoinositide production are increased in cells lacking PTEN, and this leads to parallel alterations in actin polymerization. In gradients, the normal localization of PH_{Crac}-GFP is dramatically broadened, and the region from which F actin-filled pseudopodia are extended is correspondingly increased. All of these observations suggest that

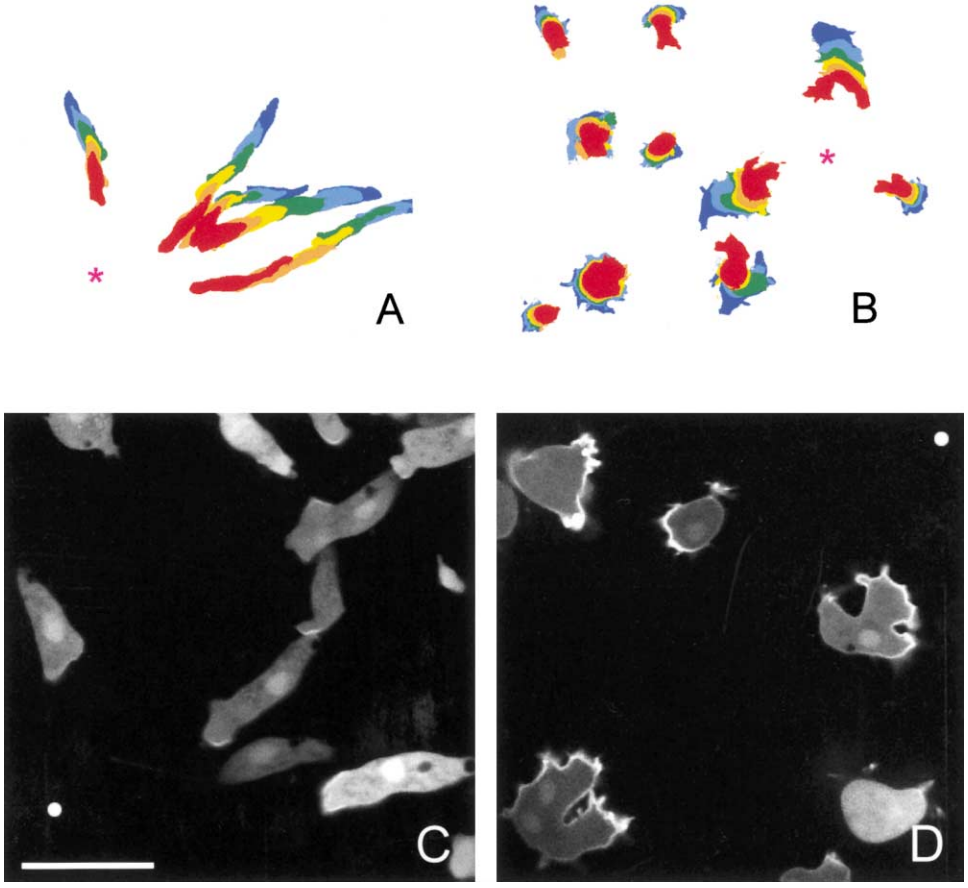

Figure 6. Chemotactic Responses of Wild-Type and *pten*$^-$ Cells

Outlines of cells moving toward micropipette filled with 1 μM cAMP were prepared at 1 min intervals and overlaid as different colors. The movements were calculated by tracing the movement of individual cell in videos. Speed is the distance between successive cell centers divided by the time-lapse interval. Chemotactic index is the cosine of the angle between the line from the centroid of the cell to the needle and a line through the direction of cell movement. The images of PH domain localization in chemotactically moving cells are taken with a confocal microscope. The asterisk or the dot indicates the position of the micropipette. (A) and (C) are wild-type cells; (B) and (D) are *pten*$^-$ cells. Calibration bar indicates 15 μm. Supplemental Videos S6C and S6D, available at http://www.cell.com/cgi/content/full/109/5/599/DC1, show the complete sequence from which the images were taken. Frames were captured at 3 s intervals and played back at 0.2 s intervals.

the inability to restrict the activity of the cytoskeletal events to the leading edge of the cell underlies the observed chemotactic defects in the *pten*$^-$ cells.

Additional responses dependent on phosphoinositides and PH domain containing proteins are probably altered in the *pten*$^-$ cells. For instance, the magnitude of the adenylyl cyclase response is greater. This increase is anticipated since activation of the adenylyl cyclases depends on Crac and significantly more Crac is recruited to the membrane in the *pten*$^-$ cells (Lilly and Devreotes, 1995). The increased adenylyl cyclase activation response in the *pten*$^-$ cells most likely leads to increased cAMP accumulation and interference with normal cell-cell communication. Careful inspection of the supplemental videos, available at http://www.cell.com/cgi/content/full/109/5/599/DC1, suggests a deficiency in the cAMP oscillators at the centers of aggregates. The oscillator involves positive feedback, reversible adaptation, and signal degradation (Devreotes et al., 1983; Parent and Devreotes, 1996). Mathematical simulations have shown that oscillations are permitted when each of these activities resides within a fixed range. We surmise that the exaggerated adenylyl cyclase activity perturbs the system so that continuous oscillations cannot be sustained. In the video, one or a few waves are typically fired before the center falls silent. However, these aberrant oscillations would not have affected our chemotaxis measurements. We monitored chemotactic behavior to externally applied gradients in the presence and absence of inhibitors of adenylyl cyclase activation and observed similar defects. We expect that protein kinase B is also more strongly activated in the *pten*$^-$ cells since its activation is controlled by recruitment to the membrane by $PI(3,4,5)P_3$ and $PI(3,4)P_2$ (Meili et al., 1999). It would be interesting to investigate the contribution of this increased activation to the phenotype.

Attempts to interfere with the PI3K activity have not provided unambiguous support for the hypothesis that phosphoinositides are a key intermediate in chemotaxis. In *D. discoideum*, neither *pi3k1*$^-$/*pi3k2*$^-$ cells nor cells treated with reasonable concentrations of PI3K inhibitors display strong defects in chemoattractant-induced actin polymerization even though increases in phosphoinositides are significantly reduced (Zhou et al., 1998).

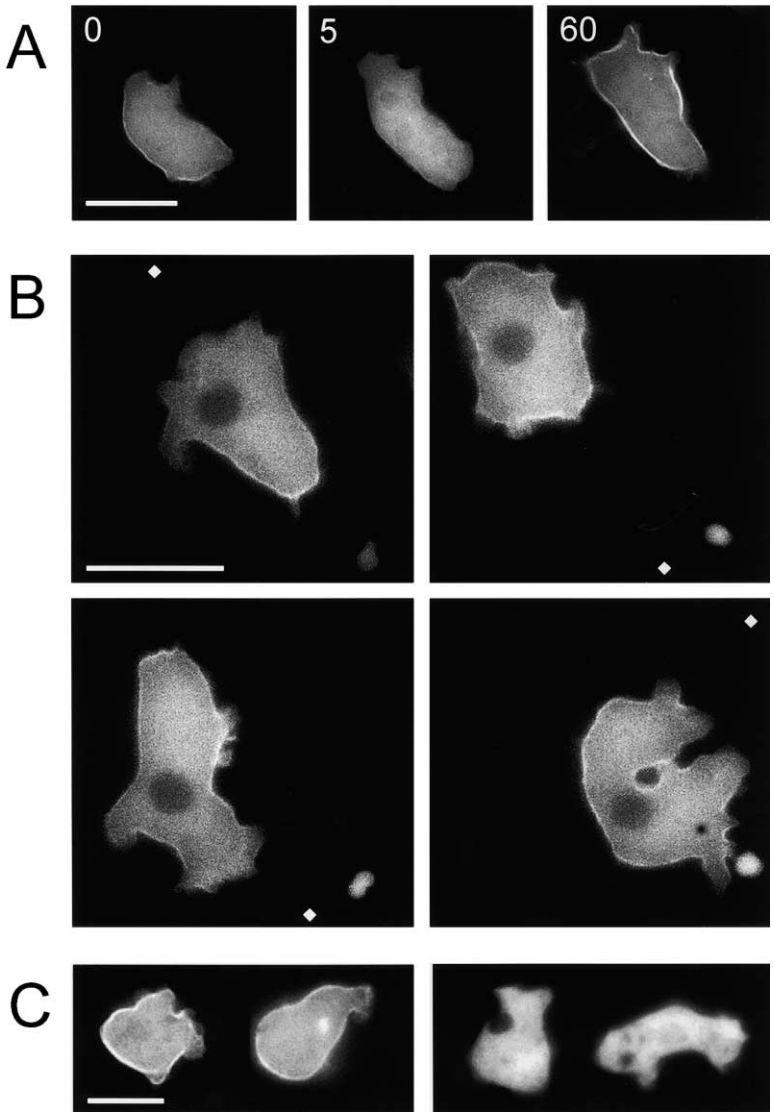

Figure 7. Subcellular Localization of PTEN-GFP in *pten*$^-$ Cells

(A) *Pten*$^-$ cells expressing PTEN-GFP were uniformly stimulated by 1 μM cAMP. Before stimulation, a detectable amount of PTEN-GFP is localized on the plasma membrane. This percentage is based on the fluorescent signal located at the cell perimeter. The actual percentage on the membrane would be calculated to be higher depending on the cell shape. Cells were stimulated with cAMP and images were captured at 5 s intervals.

(B) PTEN-GFP was accumulated in the rear of the PTEN/*pten*$^-$ cells chemotaxing toward a 1 μM cAMP filled micropipette. In this series, the micropipette was repositioned three times as indicated by the white diamonds. In upper left, the image was captured 80 s after placing the pipette. In upper right and lower left, images were captured at 125 s and 185 s, respectively, after repositioning the pipette. In lower right, the image was captured 45 s after repositioning the pipette. Calibration bar indicates 15 μm. Supplemental Video S7B available at http://www.cell.com/cgi/content/full/109/5/599/DC1 shows the complete sequence from which the images were taken. Frames were captured at 5 s intervals and played back at 0.125 s intervals.

(C) Images show the distribution of wild-type PTEN-GFP (left) and PTEN-GFP lacking the N-terminal 16 amino acids (right). Images are representative of over 50 cells that were examined.

The inhibitors decrease cell polarization and motility and do not specifically alter directional sensing. In mice lacking PI3K$_\gamma$, neutrophils display defects in chemotaxis assays, but again it is difficult to separate inhibitory effects on motility (Hirsch et al., 2000; Li et al., 2000; Sasaki et al., 2000). Moreover, chemotaxis in lymphocytes is minimally affected, and chemokine-elicited actin polymerization responses are not significantly perturbed in neutrophils or lymphocytes. The incomplete effects of the disruptions and inhibitors could possibly be due to the presence of multiple PI3K subtypes or alternate pathways for phosphoinositide production (Vanhaesebroeck et al., 2001). It seems that a portion of the chemoattractant-stimulated actin polymerization response requires only very small changes in the phosphoinositides and yet, as we show here, these lipids significantly enhance the response when they are elevated.

Studies have indicated that PTEN specifically dephosphorlylates the D3 position of phosphoinositides and thereby controls numerous physiological processes (Maehama and Dixon, 1998). The lipid phosphatase activity of PTEN, which opposes PI3K and downregulates AKT/PKB, is essential for its tumor suppressor function (Haas-Kogan et al., 1998; Myers et al., 1998; Stambolic et al., 1998). In typical cancer cell lines lacking PTEN and in cells derived from PTEN knockout mice, the levels of PI(3,4)P_2 and PI(3,4,5)P_3 are increased (Stambolic et al., 1998; Sun et al., 1999). The loss of functional PTEN leads to many abnormalities such as enhanced proliferation and decreased sensitivity to apoptotic signals (Maehama et al., 2001). The gene we have designated as PTEN and disrupted is highly homologous to its human counterpart. Furthermore, a point mutation G129E corresponding to that which causes a specific loss of lipid phosphatase activity in the human enzyme abrogates the ability of the *D. discoideum* enzyme to regulate PI(3,4,5)P_3 and PI(3,4)P_2 levels in cells (Myers et al., 1998 and data not shown)

Previous studies have suggested that cells lacking PTEN are flatter and have increased activity of the cytoskeleton around the perimeter (Tamura et al., 1998;

Liliental et al., 2000). Some studies also suggested that the cells were more motile although directional motility was not examined. We find, as others have found (Tamura et al., 1998; Liliental et al., 2000), that PTEN loss causes cells to more actively extend pseudopods. However, since the cells lose their ability to sense and respond appropriately to gradients, their directional chemotactic responses are slower. Moreover, stimulated actin polymerization is prolonged and exaggerated. It is possible that similar defects would be observed in mammalian cells if these features of chemotaxis were assessed.

The regulation and subcellular distribution of PTEN activity has not been extensively characterized. The crystal structure of human PTEN showed that the C-terminal region contained a C2 domain, which is thought to bind to membranes (Lee et al., 1999). The C-terminal regions of the *D. discoideum* and human genes are quite homologous, but we have not been able to specifically define a C2 domain. The N-terminal region of PTEN contains a putative $PI(4,5)P_2$ binding motif, suggesting a membrane localization. However, subcellular localization of mammalian PTEN indicates it predominantly distributes throughout the cytoplasm (Whang et al., 1998; Wu et al., 2000b). In these experiments, it is possible that overexpression of the protein masked its normal distribution. Our data show that a fraction of the PTEN-GFP localizes to the plasma membrane and that the N-terminal $PI(4,5)P_2$ binding motif is required for this association. Upon uniform chemoattractant stimulation, the protein rapidly dissociates from the membrane and gradually returns as the cells adapt to the stimulus. When cells are exposed to a gradient, the protein dissociates from the membrane on the side of the cell facing the higher concentration of chemoattractant. During chemotaxis, the PTEN-GFP dissociates from the membrane at the leading edge of the cell and accumulates at the rear. These behaviors are the exact opposite of those of the PH domain, indicating that the change in PTEN distribution regulates the transient increase in phosphoinositides and localizes the response to a gradient. It is interesting to speculate that the dissociation of PTEN from the membrane is caused by a decrease in $PI(4,5)P_2$ levels which may occur upon stimulation. This would comprise a feedback loop that might amplify the response. A separate feedback loop whereby $PI(3,4,5)P_3$ leads to activation of PI3K has also been proposed (Niggli, 2000). These two feedback loops may act in concert to generate a highly amplified signal.

The cells lacking PTEN activity are defective in both polarization and directional sensing, suggesting that similar biochemical mechanisms underlie both processes. The *pten*$^-$ cells are able to weakly sense the direction of a chemotactic gradient since membrane-associated phosphoinositides, reflected as PH_{Crac}-GFP binding, are broadly distributed to the front half of the cell. In addition, the large activation of physiological responses in *pten*$^-$ cells induced by uniform stimulation eventually subsides. This implies that the phosphoinositide synthetic activity (i.e., PI3K activity) must still be regulated in the *pten*$^-$ cells and that other lipid-degrading enzymes (such as PI 4- or PI 5-phosphatase) operate to remove phosphoinositides. This regulation of PI3K activity is apparently sufficient to mediate rudimentary directional sensing in the absence of PTEN function. In polarized cells, chemoattractant receptors are uniformly distributed on the membrane (Xiao et al., 1997; Servant et al., 1999). However, G protein β subunits are localized in a shallow anterior-posterior gradient (Jin et al., 2000), and there is a faster frequency of receptor-chemoattractant interaction at the front of a polarized cell (Ueda et al., 2001). The accumulation of PTEN-GFP at the rear of a cell is expected to influence the distribution of phosphoinositides on the cell membranes and may therefore also strongly contribute to polarization. Indeed, PTEN shares homology with tensin, suggesting it might associate with cytoskeletal components. Thus, polarization may result from a spontaneous redistribution of the same signal transduction components that are involved in directional sensing.

Experimental Procedures

Cell Growth and Development

Wild-type AX2 and *pten*$^-$ cells were cultured axenically in HL5 medium (Cocucci and Sussman, 1970) at 22°C. Transformants carrying PH_{Crac}-GFP and PTEN-GFP expression constructs were grown in HL5 medium containing 40 μg/ml G418 sulfate. These strains were also grown on nutrient SM agar plates with *Klebsiella aerogenes*. To assess developmental phenotypes, cells growing exponentially in HL5 medium were washed twice in development buffer (DB) and plated on 1.5% nonnutrient DB agar at 1×10^6 cells/cm^2. To determine plaque size, cells were plated as individual clones with *K. aerogenes* on SM agar plates and cultured at 22°C for 5 days.

Construction of *pten*$^-$ Cells

The accession number for the PTEN gene is AF483827. To construct the PTEN disruption vector, genomic DNA was amplified using primers P195 (5′-GCAATGGGATTTCCAAGTGAAAAGTTG-3′) and P1614 (5′-TGATGGGTTTGATTCTTGTTGTACAGGG-3′) located in the PTEN coding region and cloned into the TA cloning vector pCR2.1 (Invitrogen). Blasticidin S resistance (BSR) cassette from pBsrΔBam (Adachi et al., 1994) was inserted into the Hinc II site of the PTEN genomic fragment (P195:P1614) and then digested with appropriate restriction enzymes to remove the vector backbone sequence. The linearized disruption vector (10 μg) was introduced into growth-phase AX2 cells by electroporation using a Bio-Rad gene pulser. Transformants were selected in HL5 containing 10 μg/ml Blasticidin S sulfate on plastic dishes. After 5 days, cells were harvested and cloned on SM-agar plates containing 10 μg/ml of Blasticidin S with *K. aerogenes*. Resultant colonies were picked and checked for disruption of respective genes by PCR and Southern blot analysis. The formal gene and strain nanes for PTEN gene and these *pten*$^-$ cells are proposed as *ptnA* and *ptnA*−.

Construction of the GFP Fusion Protein Expression Vector and Transformation of Cells

The full-length PTEN cDNA sequence was amplified by PCR using primers P111 (5′-GGAGATCTGGAAACAAATAGAATGAG-3′), which created a Bgl II site at the 5′ end and P1664 (5′-CCCTCGAGTCTGC TTCAACCTTTGGAGC-3′), which created a XhoI site at the 5′ end, and cloned upstream of the start codon of the GFP gene. The resulting PTEN-GFP construct was sequenced and finally cloned downstream of the actin 15 promoter of the *D. discoideum* extrachromosomal vector pJK1 (Pitt et al., 1992). For the expression of PH_{Crac}-GFP, the PH domain from CRAC was ligated upstream of the GFP gene and expressed from actin 15 promoter (Jin et al., 2000). These vectors (10 μg) were introduced into growth phase cells by electroporation. Transformants were selected in HL5 containing 10 μg/ml G418. After 7 days, when colonies were visible, cells were harvested and observed for GFP expression under a fluorescence microscope.

Chemotaxis Assay

Cells grown in shaking culture were washed twice with DB, resuspended at 2×10^7 cells/ml in shaking, and induced to differentiate

with 100 nM cAMP pulses at 6 min intervals for 5 hr (Devreotes et al., 1987). The small-drop chemotaxis assay was performed as described (Konijn, 1970; van Haastert and Konijn, 1982). Small droplets (0.1 μl) having 100–200 differentiated cells were spotted on 1.5% DB agar plates containing 3 mM caffeine. Different doses of cAMP solution were spotted close to the drops of cells. After 30–60 min in a humidified chamber, chemotactic responses were observed and scored positive if at least twice as many cells were pressed against the edge closest to the cAMP droplet as to the opposite side. Chemotactic movements of cells to a micropipette containing cAMP were performed as described (Parent et al., 1998). Differentiated cells were plated on a chambered coverglass (Lab-Tek, Nalge Nunc) and allowed to adhere to the surface. A micropipette filled with 1 μM cAMP was positioned and images of moving cells were recorded.

Actin Polymerization, Adenylyl Cyclase, and cGMP Accumulation Assays

Differentiated cells were diluted to 1×10^7 cells/ml and shaken at 200 rpm with 2 mM caffeine for 30 min. Cells were collected, washed twice, resuspended at 3×10^7 cells/ml in PM with 3 mM caffeine, and shaken at room temperature for 10 min. At various time points after addition of 1 μM cAMP, cells were fixed and stained with TRITC-phalloidin to measure the amounts of F actin as described (Kim et al., 1997). For adenylyl cyclase assay, cells were stimulated at 8×10^7 cells/ml with 1 μM cAMP and lysed through the 5 μm pore size nucleopore filters into a reaction mixture containing [α-^{32}P]ATP. The amount of [^{32}P]cAMP synthesized in 1 min was measured as described (Theibert and Devreotes, 1986). To measure the guanylyl cyclase activation, cells at 5×10^7 cells/ml were stimulated with 1 μM cAMP. At designated times, reactions were terminated by the addition of perchloric acid and cGMP accumulation was counted by a competitive radioimmunoassay, [^{3}H]GMP detection kit (Amersham).

Fluorescence Microscopy Analysis on Living Cells

Images of the living cells were observed using an inverted Zeiss microscope (Axiovert 135 TV) or confocal laser scanning microscope (Perkin Elmer UltraView) with an inverted microscope (Nikon).

Immunoblot Analysis of PH Domain Translocation Assay

Cells were pretreated with caffeine as described above, washed, and resuspended in PM. Cells were stimulated with 1 μM cAMP and at indicated time points, filter-lysed into ice-cold PM to terminate the reaction. Membrane fractions were collected by centrifugation at 15,000 × g for 1 min and subjected to assay by immunoblot of PH_{Crac}-GFP with anti-GFP antibody (BABCO). Quantification was performed with NIH Image software.

Acknowledgments

This work was supported by NIH grants GM34933 and 57874 to P.N.D. The authors wish to thank Linnan Tang for constructing the Supplemental Video S7 and Chris Janetopoulos for assistance in fluorescence microscopy.

Received: December 20, 2001
Revised: March 4, 2002

References

Adachi, H., Hasebe, T., Yoshinaga, K., Ohta, T., and Sutoh, K. (1994). Isolation of *Dictyostelium discoideum* cytokinesis mutants by restriction enzyme-mediated integration of the blasticidin S resistance marker. Biochem. Biophys. Res. Commun. *205*, 1808–1814.

Baggiolini, M. (2001). Chemokines in pathology and medicine. J. Intern. Med. *250*, 91–104.

Buczynski, G., Grove, B., Nomura, A., Kleve, M., Bush, J., Firtel, R.A., and Cardelli, J. (1997). Inactivation of two *Dictyostelium discoideum* genes, DdPIK1 and DdPIK2, encoding proteins related to mammalian phosphatidylinositide 3-kinases, results in defects in endocytosis, lysosome to postlysosome transport, and actin cytoskeleton organization. J. Cell Biol. *136*, 1271–1286.

Cocucci, S.M., and Sussman, M. (1970). RNA in cytoplasmic and nuclear fractions of cellular slime mold amebas. J. Cell Biol. *45*, 399–407.

Devreotes, P.N., Potel, M.J., and MacKay, S.A. (1983). Quantitative analysis of cyclic AMP waves mediating aggregation in *Dictyostelium discoideum*. Dev Biol. *96*, 405–415.

Devreotes, P., Fontana, D., Klein, P., Sherring, J., and Theibert, A. (1987). Transmembrane signaling in *Dictyostelium*. Methods Cell Biol. *28*, 299–331.

Funamoto, S., Milan, K., Meili, R., and Firtel, R.A. (2001). Role of phosphatidylinositol 3′ kinase and a downstream pleckstrin homology domain-containing protein in controlling chemotaxis in *Dictyostelium*. J. Cell Biol. *153*, 795–810.

Goberdhan, D.C., Paricio, N., Goodman, E.C., Mlodzik, M., and Wilson, C. (1999). *Drosophila* tumor suppressor PTEN controls cell size and number by antagonizing the Chico/PI3-kinase signaling pathway. Genes Dev. *13*, 3244–3258.

Haas-Kogan, D., Shalev, N., Wong, M., Mills, G., Yount, G., and Stokoe, D. (1998). Protein kinase B (PKB/Akt) activity is elevated in glioblastoma cells due to mutation of the tumor suppressor PTEN/MMAC. Curr. Biol. *8*, 1195–1198.

Haugh, J.M., Codazzi, F., Teruel, M., and Meyer, T. (2000). Spatial sensing in fibroblasts mediated by 3′ phosphoinositides. J. Cell Biol. *151*, 1269–1280.

Hirsch, E., Katanaev, V.L., Garlanda, C., Azzolino, O., Pirola, L., Silengo, L., Sozzani, S., Mantovani, A., Altruda, F., and Wymann, M.P. (2000). Central role for G protein-coupled phosphoinositide 3-kinase γ in inflammation. Science *287*, 1049–1053.

Janetopoulos, C., Jin, T., and Devreotes, P. (2001). Receptor-mediated activation of heterotrimeric G proteins in living cells. Science *291*, 2408–2411.

Jin, T., Zhang, N., Long, Y., Parent, C.A., and Devreotes, P.N. (2000). Localization of the G protein βγ complex in living cells during chemotaxis. Science *287*, 1034–1036.

Kim, J.Y., Soede, R.D., Schaap, P., Valkema, R., Borleis, J.A., Van Haastert, P.J., Devreotes, P.N., and Hereld, D. (1997). Phosphorylation of chemoattractant receptors is not essential for chemotaxis or termination of G-protein-mediated responses. J. Biol. Chem. *272*, 27313–27318.

Kim, C.H., Hangoc, G., Cooper, S., Helgason, C.D., Yew, S., Humphries, R.K., Krystal, G., and Broxmeyer, H.E. (1999). Altered responsiveness to chemokines due to targeted disruption of SHIP. J. Clin. Invest. *104*, 1751–1759.

Konijn, T.M. (1970). Microbiological assay of cyclic 3′,5′-AMP. Experientia *26*, 367–369.

Lee, J.O., Yang, H., Georgescu, M.M., Di Cristofano, A., Maehama, T., Shi, Y., Dixon, J.E., Pandolfi, P., and Pavletich, N.P. (1999). Crystal structure of the PTEN tumor suppressor: implications for its phosphoinositide phosphatase activity and membrane association. Cell *99*, 323–334.

Levchenko, A., and Iglesias, P.A. (2002). Models of eukaryotic gradient sensing: application to chemotaxis of amoebae and neutrophils. Biophys. J. *82*, 50–63.

Li, Z., Jiang, H., Xie, W., Zhang, Z., Smrcka, A.V., and Wu, D. (2000). Roles of PLC-β2 and -β3 and PI3Kγ in chemoattractant-mediated signal transduction. Science *287*, 1046–1049.

Liliental, J., Moon, S.Y., Lesche, R., Mamillapalli, R., Li, D., Zheng, Y., Sun, H., and Wu, H. (2000). Genetic deletion of the Pten tumor suppressor gene promotes cell motility by activation of Rac1 and Cdc42 GTPases. Curr. Biol. *10*, 401–404.

Lilly, P.J., and Devreotes, P.N. (1995). Chemoattractant and GTP γ S-mediated stimulation of adenylyl cyclase in *Dictyostelium* requires translocation of CRAC to membranes. J. Cell Biol. *129*, 1659–1665.

Maehama, T., and Dixon, J.E. (1998). The tumor suppressor, PTEN/MMAC1, dephosphorylates the lipid second messenger, phosphatidylinositol 3,4,5-trisphosphate. J. Biol. Chem. *273*, 13375–13378.

Maehama, T., Taylor, G.S., and Dixon, J.E. (2001). PTEN and myotubularin: novel phosphoinositide phosphatases. Annu. Rev. Biochem. *70*, 247–279.

Meili, R., Ellsworth, C., Lee, S., Reddy, T.B., Ma, H., and Firtel, R.A.

(1999). Chemoattractant-mediated transient activation and membrane localization of Akt/PKB is required for efficient chemotaxis to cAMP in *Dictyostelium*. EMBO J. *18*, 2092–2105.

Myers, M.P., Pass, I., Batty, I.H., Van der Kaay, J., Stolarov, J.P., Hemmings, B.A., Wigler, M.H., Downes, C.P., and Tonks, N.K. (1998). The lipid phosphatase activity of PTEN is critical for its tumor supressor function. Proc. Natl. Acad. Sci. USA *95*, 13513–13518.

Niggli, V. (2000). A membrane-permeant ester of phosphatidylinositol 3,4,5-trisphosphate (PIP(3)) is an activator of human neutrophil migration. FEBS Lett. *473*, 217–221.

Ogg, S., and Ruvkun, G. (1998). The *C. elegans* PTEN homolog, DAF-18, acts in the insulin receptor-like metabolic signaling pathway. Mol. Cell *2*, 887–893.

Parent, C.A., and Devreotes, P.N. (1996). Molecular genetics of signal transduction in *Dictyostelium*. Annu. Rev. Biochem. *65*, 411–440.

Parent, C.A., and Devreotes, P.N. (1999). A cell's sense of direction. Science *284*, 765–770.

Parent, C.A., Blacklock, B.J., Froehlich, W.M., Murphy, D.B., and Devreotes, P.N. (1998). G protein signaling events are activated at the leading edge of chemotactic cells. Cell *95*, 81–91.

Pitt, G.S., Milona, N., Borleis, J., Lin, K.C., Reed, R.R., and Devreotes, P.N. (1992). Structurally distinct and stage-specific adenylyl cyclase genes play different roles in *Dictyostelium* development. Cell *69*, 305–315.

Rickert, P., Weiner, O.D., Wang, F., Bourne, H.R., and Servant, G. (2000). Leukocytes navigate by compass: roles of PI3Kγ and its lipid products. Trends Cell Biol. *10*, 466–473.

Sasaki, T., Irie-Sasaki, J., Jones, R.G., Oliveira-dos-Santos, A.J., Stanford, W.L., Bolon, B., Wakeham, A., Itie, A., Bouchard, D., Kozieradzki, I., et al. (2000). Function of PI3Kγ in thymocyte development, T cell activation, and neutrophil migration. Science *287*, 1040–1046.

Servant, G., Weiner, O.D., Neptune, E.R., Sedat, J.W., and Bourne, H.R. (1999). Dynamics of a chemoattractant receptor in living neutrophils during chemotaxis. Mol. Biol. Cell *10*, 1163–1178.

Servant, G., Weiner, O.D., Herzmark, P., Balla, T., Sedat, J.W., and Bourne, H.R. (2000). Polarization of chemoattractant receptor signaling during neutrophil chemotaxis. Science *287*, 1037–1040.

Stambolic, V., Suzuki, A., de la Pompa, J.L., Brothers, G.M., Mirtsos, C., Sasaki, T., Ruland, J., Penninger, J.M., Siderovski, D.P., and Mak, T.W. (1998). Negative regulation of PKB/Akt-dependent cell survival by the tumor suppressor PTEN. Cell *95*, 29–39.

Sun, H., Lesche, R., Li, D.M., Liliental, J., Zhang, H., Gao, J., Gavrilova, N., Mueller, B., Liu, X., and Wu, H. (1999). PTEN modulates cell cycle progression and cell survival by regulating phosphatidylinositol 3,4,5,-trisphosphate and Akt/protein kinase B signaling pathway. Proc. Natl. Acad. Sci. USA *96*, 6199–6204.

Tamura, M., Gu, J., Matsumoto, K., Aota, S., Parsons, R., and Yamada, K.M. (1998). Inhibition of cell migration, spreading, and focal adhesions by tumor suppressor PTEN. Science *280*, 1614–1617.

Theibert, A., and Devreotes, P.N. (1986). Surface receptor-mediated activation of adenylate cyclase in *Dictyostelium*. Regulation by guanine nucleotides in wild-type cells and aggregation deficient mutants. J. Biol. Chem. *261*, 15121–15125.

Ueda, M., Sako, Y., Tanaka, T., Devreotes, P., and Yanagida, T. (2001). Single-molecule analysis of chemotactic signaling in *Dictyostelium* cells. Science *294*, 864–867.

van Es, S., and Devreotes, P.N. (1999). Molecular basis of localized responses during chemotaxis in amoebae and leukocytes. Cell. Mol. Life Sci. *55*, 1341–1351.

van Haastert, P.J., and Konijn, T.M. (1982). Signal transduction in the cellular slime molds. Mol. Cell. Endocrinol. *26*, 1–17.

Vanhaesebroeck, B., Leevers, S.J., Ahmadi, K., Timms, J., Katso, R., Driscoll, P.C., Woscholski, R., Parker, P.J., and Waterfield, M.D. (2001). Synthesis and function of 3-phosphorylated inositol lipids. Annu. Rev. Biochem. *70*, 535–602.

Wardlaw, A.J., Brightling, C., Green, R., Woltmann, G., and Pavord, I. (2000). Eosinophils in asthma and other allergic diseases. Br. Med. Bull. *56*, 985–1003.

Whang, Y.E., Wu, X., Suzuki, H., Reiter, R.E., Tran, C., Vessella, R.L., Said, J.W., Isaacs, W.B., and Sawyers, C.L. (1998). Inactivation of the tumor suppressor PTEN/MMAC1 in advanced human prostate cancer through loss of expression. Proc. Natl. Acad. Sci. USA *95*, 5246–5250.

Wu, D., Huang, C.K., and Jiang, H. (2000a). Roles of phospholipid signaling in chemoattractant-induced responses. J. Cell Sci. *113 (part 17)*, 2935–2940.

Wu, X., Hepner, K., Castelino-Prabhu, S., Do, D., Kaye, M.B., Yuan, X.J., Wood, J., Ross, C., Sawyers, C.L., and Whang, Y.E. (2000b). Evidence for regulation of the PTEN tumor suppressor by a membrane-localized multi-PDZ domain containing scaffold protein MAGI-2. Proc. Natl. Acad. Sci. USA *97*, 4233–4238.

Wymann, M.P., Sozzani, S., Altruda, F., Mantovani, A., and Hirsch, E. (2000). Lipids on the move: phosphoinositide 3-kinases in leukocyte function. Immunol. Today *21*, 260–264.

Xiao, Z., Zhang, N., Murphy, D.B., and Devreotes, P.N. (1997). Dynamic distribution of chemoattractant receptors in living cells during chemotaxis and persistent stimulation. J. Cell Biol. *139*, 365–374.

Zhou, K., Pandol, S., Bokoch, G., and Traynor-Kaplan, A.E. (1998). Disruption of *Dictyostelium* PI3K genes reduces [32P]phosphatidylinositol 3,4 bisphosphate and [32P]phosphatidylinositol trisphosphate levels, alters F actin distribution and impairs pinocytosis. J. Cell Sci. *111 (part 2)*, 283–294.